Research Article

Research on Pure Modes I and II and Mixed-Mode (I/II) Fracture Toughness of Geopolymer Fiber-Reinforced Concrete

Sundaravadivelu Karthik ⬡,[1] **Kaliyaperumal Saravana Raja Mohan,**[1]
Gunasekaran Murali ⬡,[1,2] **and Gobinath Ravindran** ⬡[3]

[1]*School of Civil Engineering, SASTRA Deemed University, Thanjavur 613401, India*
[2]*Division of Research & Innovation, Uttaranchal University, Dehradun 248007, India*
[3]*Department of Civil Engineering, SR University, Warangal 506371, India*

Correspondence should be addressed to Sundaravadivelu Karthik; karthik@civil.sastra.edu

The unsustainable use of resources and the rising demand for traditional concrete have disrupted ecological equilibrium, necessitating the adoption of a more appropriate and long-lasting alternative. One such substitute for cement in concrete production is geopolymer concrete, although this material is prone to cracking and fracturing due to its low tensile strength, leading to costly repairs or even structural collapse. Fiber-reinforced concrete has recently been widely adopted as a construction material to counteract these issues. This research examined the crack proliferation and fracture toughness of geopolymer concrete comprising different fibers using a cracked Brazilian disc. Four different fibers were used, such as polypropylene and steel fiber (short and long), at a dosage of 1.5% by volume. Fracture toughness was computed for various modes (I, II, and I/II) of fractures, and crack propagation from cracked specimens was studied. A different angle of inclination (0, 15, 28, 83, 60, 75, and 90 degrees) was used to conduct the Brazilian disc test on the specimens with respect to the preexisting crack direction. The findings indicate that the increasing loading angle increased the load-carrying capacity. The fracture toughness values of specimens under all three modes ranged from 0.26 to 1.75 MPa.m$^{1/2}$. Additionally, long polypropylene and steel fibers exhibit higher fracture toughness than short fibers.

1. Introduction

An excessive amount of carbon dioxide and other greenhouse gases are released due to concrete production. Therefore, scientists have been looking into possible solutions to slow the dramatic rise in atmospheric carbon dioxide levels [1]. Environmentalists and scientists have advocated the utilization of supplemental cementitious materials due to the cement industry's high carbon footprint (about one kilogram of CO_2 is released for every kilogram of cement manufactured) [2]. Cement is often supplemented with cementitious materials, mainly waste materials or industrial by products, to reduce the harmful effects on the ecosystem and natural surroundings. The concrete's durability was improved by using supplemental cementitious

materials in place of some cement, which also helped save natural resources and cut down on carbon dioxide emissions. The improvement was primarily attributable to the pozzolanic properties of supplementary cementitious materials, which caused a change in the microstructure of the cement matrix. Geopolymers, made from recycled industrial wastes, have emerged as a promising alternative to cement in current history. Because of their superior mechanical and durability properties, they leave a far smaller carbon footprint than traditional concrete [3, 4]. The utilization of geopolymer concrete made with industrial waste has increased recently in the construction sector [5–7]. Arunachelam et al. [8] reported that the geopolymer concrete made with 10 molarity raised the concrete's strength by approximately 35% when the molarity of the NaOH solution

was increased to 16 M. Additionally, the compressive strength was increased by 53.8% when river sand was replaced with 100% copper slag compared to the control geopolymer concrete made with no copper slag. The use of high-volume copper slag instead of river sand in the production of high-strength geopolymer concrete was studied by Arunachelam et al. [9]. According to the findings, the optimized geopolymer concrete mix achieved a maximum compressive strength of 79.0 MPa when 2% microsilica was added. However, brittle behavior is the main drawback of geopolymer concrete and other plain concrete as well [10, 11]. By incorporating fibers (polyethylene, polypropylene, and steel) into micromechanics-based concrete, the material's tensile behavior, tensile strain capacity, strain-hardening, and microcracking can be improved [12–15].

The configuration of crack commencement and spread in brittle materials like concrete and rocks are significant factors to consider while researching the fracturing of these materials [16]. After a crack opens, the stress condition transforms significantly close to the crack's tip. The fracture behavior of these materials has been the subject of numerous theoretical frameworks, including the empirical criterion, minimum strain energy density criterion, maximum energy release rate criterion, and maximum tangential stress criterion [17]. The geometry, crack inclination angle, and fracture mechanism close to crack tips all influence a parameter called the stress intensity factor. The loading at the crack tip and fracture surface displacement are the two factors determining the fracturing type [18]. A fracture or crack is characterized by the presence of two surfaces or borders, one of which essentially coincides with the other. According to the stress conditions, a crack can theoretically spread in three fundamental modes: (i) Mode I represents the tensile opening, characterized by opening up the crack face and separating along a direction normal to the fracture plane. (ii) The crack faces slide parallel to the direction of crack growth in mode II, which can be considered shearing or in-plane sliding at the crack tip. (iii) Mode III is known as the out-of-plane mode or tearing, in which cracks displace perpendicular to the leading edge and crack faces slide in a direction parallel to the stress. The behavior of crack growth shifts depending on the geometry and direction of the crack. Many studies have been conducted on mixed-mode fractures; nevertheless, most of these studies have concentrated on mixed-mode I-II and I-III fractures. Several experimental methods include four-point bending [19], cracked chevron-notched Brazilian discs [20], centrally cracked Brazilian discs [21], and bending at three points on a semicircular disc [22].

For instance, the fracture energy of self-consolidating concrete specimens under modes I and II was investigated by Ghomian and Dehestani [23]. In this study, they utilized two distinct specimen arrangements to compare the effects of water/cement ratios on the fracture of self-consolidating concrete under mode II. In addition, they concluded that crack extension and an improvement in the mode II fracture energy occurred when the water-cement ratio was decreased, while the compressive strength was increased. In addition, the concrete exhibited a brittle tendency, which became more pronounced as the compressive strength and specimen size increased. Erarslan [16] conducted experiments on cracked chevron-notched Brazilian concrete discs at four angles of crack inclination (0, 30, 45, and 70 degrees). The location of crack commencement moved closer to the center of the preexistent crack as the increased angle of crack inclination with respect to the loading direction. This phenomenon occurred when the angle of inclination was more than 30 degrees. Initially, cracks formed perpendicular to the plane of tensile stress, and the fracture subsequently extended in a direction parallel to loading at a $0°$ angle of inclination. The crack got progressively more curved toward the loading point with the increased angle of inclination.

In recent years, many experiments have been undertaken on reinforced concrete mixtures incorporating various fibers to enhance fracture properties. For instance, Razmi and Mirsayar [24] researched the fracture properties of fibrous concrete comprising jute fiber. Researchers investigated how the amount of jute fiber affected the tensile and flexural strengths, mixed-mode fracture toughness, and uniaxial compressive strength of the material. Mixed-mode fracture toughness was evaluated using cracked semicircular bend specimens. Their findings demonstrated that the mixed-mode fracture toughness of concrete improved as the proportion of jute fibers increased. According to Sreenath et al. [25], the fibrous reactive powder concrete, which had 30% of its cement replaced with ground granulated blast furnace slag, displayed the greatest fracture toughness. These values were 2.35 and 0.98 MPa.m$^{0.5}$ for modes I and III, respectively. Adding short macrosteel fibers greatly enhanced mode I fracture toughness. On the other hand, it did not help very much when mode III loadings were considered. Positive interaction between hybrid fiber combinations (glass, polypropylene, and steel) in geopolymer concrete was found by Asrani et al. [26], which increased fracture energy by as much as 15.72 N/mm. Compared to Brazilian notched discs, it was discovered that fracture toughness was significantly improved when double-notched cubes were used instead. A disc and cube specimen comparison revealed a normalized fracture toughness ratio of 0.37 to 0.47, respectively.

Fracture toughness evolution in pure modes I and II and mixed modes is significant for structural design, yet little information is provided on this topic in the literature. However, no prior research has used cracked Brazilian disc specimens to investigate the effects of mixed-mode loading on the fracture toughness and crack propagation of geopolymer concrete. Thus, this study aims to evaluate the fracture toughness of geopolymer fibrous concrete under pure modes I and II and a mixed mode (I/II). The centrally cracked Brazilian disc specimens with four different fibers, such as polypropylene and steel fiber (short and long), at a dosage of 1.5% each by volume, were tested to predict fracture toughness and crack spread. In addition, mode I-II and mixed-mode (I/II) fracture toughness was determined, and crack spread from preexisting cracks in the specimens was also computed. A different angle of inclination (0, 15, 28, 83, 60, 75, and 90 degrees) was used to perform the Brazilian disc test on the geopolymer concrete specimens with respect

to the preexisting crack direction. Investigations on the effects of various fibers on mode I, mode II, and (I/II) fracture toughness and crack spreading were conducted concurrently. Based on the available research, Brazilian disc tests have been conducted to determine the fracture toughness and spreading of cracks in nonfibrous concrete, mortars, and rocks. The novelty of this research is in the testing of geopolymer concrete specimens reinforced with four different fibers besides the nonfibrous geopolymer concrete.

2. Materials and Methods

2.1. Raw Materials

(i) Neyveli Lignite Corporation supplied class F fly ash (FA) for use in the binder, which was employed in accordance with the specifications set out by ASTM C618-08 [27]. The fabricated specimens were cured at room temperature during the process of making geopolymer concrete. The silica fume (SF), ground granulated blast furnace slag (GGBFS), and FA were combined to make the combination used to make the geopolymer concrete. Previous studies have demonstrated that increasing GGBFS and CaO concentrations can hasten the polymerization process [28]. Another possible mechanism for forming a dense matrix is the rapid reaction of silica fumes with an alkaline solution, resulting from the smaller particle size of silica fumes [28]. Astra Chemicals, Chennai, was the supplier of the alkaline solutions, including GGBFS and SF. The raw materials utilized in this investigation are illustrated in Figure 1. The chemical characteristics of GGBFS, FS, and SF are presented in Table 1.

(ii) In accordance with the specifications found in IS: 383 [29], the fine aggregate consisted of river sand with less than 2.36 mm in size, a specific gravity of 2.65, and a fineness modulus of 2.41. According to IS 383 [29], the coarse aggregate comprised crushed granite gravel with a particle size of 12.5 mm. The specific gravity of the coarse aggregate was 2.69, and its water absorption was 0.56%. The bulk density of the coarse aggregate was 1700 kg/m^3. The particle size distribution of the used aggregates is shown in Figure 2.

(iii) A commercially available superplasticizer (Tech Mix 550) was utilized at a dosage of 1.5% by binder weight to create flowable geopolymer concrete.

(iv) A combination of sodium silicate (Na_2SiO_3) and sodium hydroxide (NaOH) was used to activate the pozzolanic binders.

(v) Fibers of varying lengths and types were utilized, including short and long polypropylene fiber and short and long steel fiber. Figure 3 depicts the four distinctive fiber appearances, and Table 2 demonstrates the fiber properties. In order to study the efficiency of fiber types and lengths in fracture

TABLE 1: Chemical composition of binders.

Oxide	Class F FA	GGBFS	SF
(TiO$_2$, %)	0.1	—	—
(Na$_2$O, %)	0.2	—	—
(K$_2$O, %)	1.6	—	—
(MgO, %)	5.9	8.9	0.6
(CaO, %)	6.4	34.62	—
(Fe$_2$O$_3$, %)	9.8	1	0.3
(Al$_2$O$_3$, %)	25	17.2	0.6
(SiO$_2$, %)	51	36.7	92.8
(LOI, %)	2.6	1.92	1.28

toughness, two types of fiber, such as polypropylene fiber (PF) and steel fiber (SF), were selected in this study. When the fiber length is less than or equal to 30 mm, it is categorized as a short fiber in this study.

2.2. Mixing and Preparation of the Specimen. Table 3 displays the mixing combinations used in this investigation, including binder material, fine and coarse aggregates, and fibers. Multiple trial tests were conducted using all these material combinations to ensure a compressive strength of over 30 MPa. Alkaline solutions were made by dissolving sodium hydroxide pellets in distilled water until they reached the desired molar concentration. Afterwards, sodium silicate was added to produce an alkaline solution. The specimen casting solution was prepared and kept one day in advance. In this particular investigation, the ratio of Na_2SiO_3/NaOH was set at 1.5 and the molar concentration was 12. These proportions result from numerous iterations of the compressive strength test, from which the results were compiled in our earlier study [28]. The procedure for producing geopolymer concrete begins with combining and mixing of dry materials such as FA, SF, and GGBFS for two minutes; after that, the fine aggregate is included in the mixture and allowed to mix for two minutes. After this, coarse aggregates and fibers were included in the mixture and allowed to blend for an extended period until the fibers were evenly dispersed throughout the mixture. After adding the alkaline solutions to dry ingredients, the mixture was thoroughly combined by mixing for additional 3 minutes. The wet mixture of the GPC is shown in Figure 4(a). Casting all geopolymer concrete specimens within 5 minutes ensured that the concrete was compacted and dense throughout. Before beginning the testing procedure, fabricated specimens were cured at room temperature with a relative humidity of 72% and temperatures ranging between 26 and 30°C for 28 days after demoulding. Figure 4(b) depicts the centrally cracked specimens after casting, while Figure 4(c) depicts the demolded specimens. Several centrally cracked Brazilian disc specimens were prepared to evaluate the fracture toughness and arranged in the laboratory before testing (Figure 4(d)).

Five different geopolymer concrete mixtures were prepared with and without fibers. The first mixture, which included no fibers and was labelled GPC, served as the control specimen. The second and third mixture of GPC was reinforced with short and long polypropylene fibers, labelled

FIGURE 1: Raw materials: (a) silica fume, (b) GGBFS, (c) fly ash, (d) fine aggregate, (e) coarse aggregate, (f) superplasticizer, (g) sodium silicate, and (h) sodium hydroxide.

TABLE 2: Information about the properties of fibers.

Properties/Fiber type	Short fiber		Long fiber	
	Polypropylene	Steel	Polypropylene	Steel
Length (mm)	13	30	45	50
Diameter (mm)	0.01	0.5	0.8	1
Tensile strength (MPa)	360	1200	500	1150
Aspect ratio	1300	60	56.25	50

TABLE 3: Mixing composition.

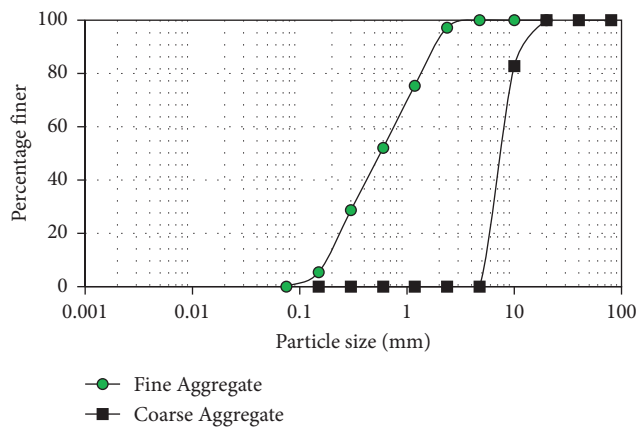| Mixture id	FA (kg/m³)	GGBFS (kg/m³)	SF (kg/m³)	Fine agg. (kg/m³)	Coarse agg. (kg/m³)	Na₂SiO₃ (kg/m³)	NaOH (kg/m³)	Fiber type	Fiber dosage (%) by volume
GPC								—	0
G-SPF								SPF	1.5
G-LPF	184	184	41	554	1294	101	70	LPF	1.5
G-SSF								SSF	1.5
G-LSF								LSF	1.5

FIGURE 2: Aggregate particle size distribution.

G-SPF and G-LPF, respectively. The final two mixtures were prepared with short and long polypropylene fibers, labelled G-SSF and G-LSF, respectively. Regardless of fiber types, all the GPC specimens were reinforced with a 1.5% dosage, and their diameter and thickness were 150 and 25 mm, respectively. A different angle of inclination (0, 15, 28, 83, 60, 75, and 90°) was used to evaluate the fracture toughness of the specimens with respect to the preexisting crack direction.
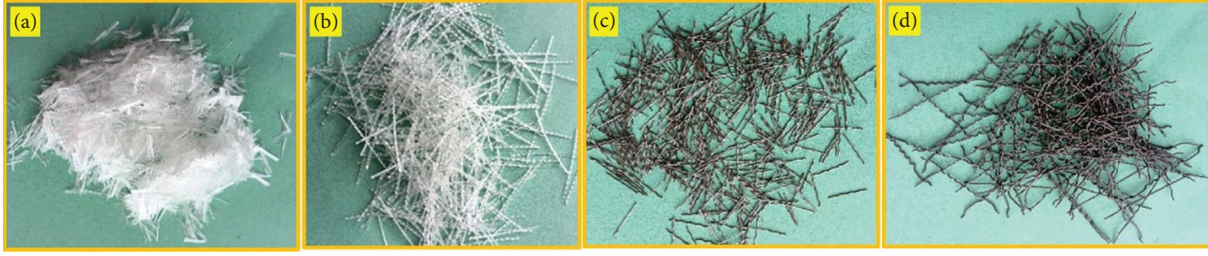
FIGURE 3: The four distinctive fiber appearances: (a) short PF, (b) long PF, (c) short SF, and (d) long SF.
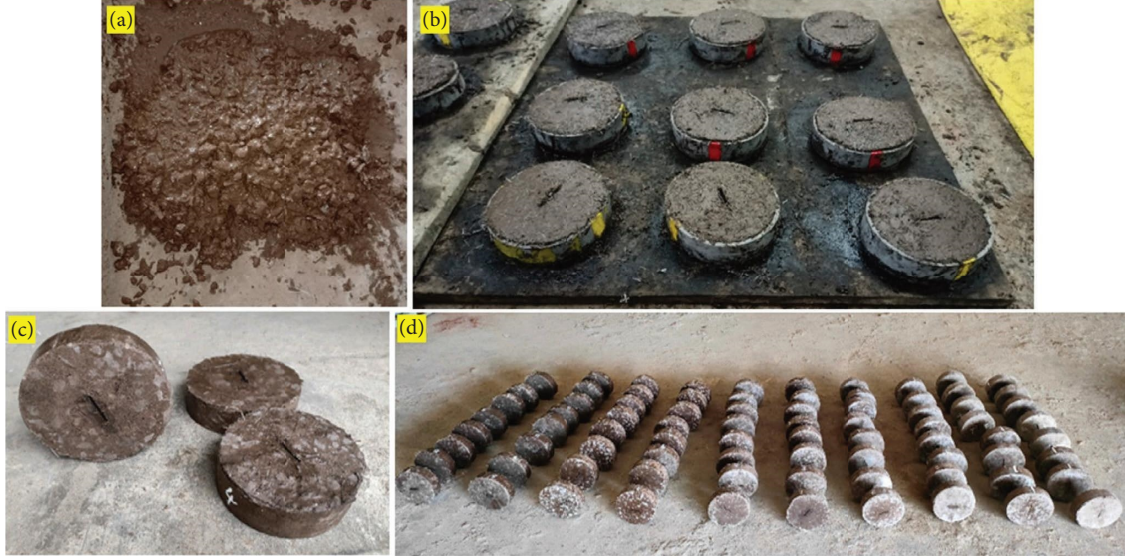

FIGURE 4: (a) Geopolymer mixture, (b) cast specimen with a notch, (c) demolded specimen, and (d) number of specimens before testing.

2.3. Experimental Setup. The Brazilian tensile and uniaxial compressive strengths were measured using universal testing equipment. The mixed-mode fracture of different specimens, including marble, plaster, and graphite, was the motivation behind the development of this test by Awaji and Sato [30]. The fracture toughness in modes I, II, and mixed I/II was determined by solving equations (1)–(5) [21]. The Brazilian disc, which has a thickness of 40 mm and a diameter of 150 mm, was used in this study. The precrack in the middle is an average of 30 mm in length, 1.5 mm in width, and 40 mm in depth, which is equivalent to the disc thickness (Figure 5):

$$K_{IC} = \frac{P_{max} \sqrt{a}}{\sqrt{\pi R t}} B_I,\tag{1}$$

$$B_I = 1 - 4 \sin^2 \beta + 4 \sin^2 \beta \left(1 - 4 \cos^2 \beta\right)\left(\frac{a}{R}\right)^2,\tag{2}$$

$$K_{IIC} = \frac{P_{max} \sqrt{a}}{\sqrt{\pi R t}} B_{II},\tag{3}$$

$$B_{II} = \left[2 + \left(8 \cos^2 \beta - 5\right)\left(\frac{a}{R}\right)^2\right] \sin 2\beta,\tag{4}$$

$$K_{eff} = \sqrt{K_{IC}^2 + K_{IIC}^2},\tag{5}$$

where β is the angle of the crack with respect to the direction in which the load is applied, a represents half the crack's length, t is the disc's thickness, R is the radius of the disc, and P_{max} is the maximum load before a fracture occurs. Fracture toughness is measured in K_{IC} for mode I and K_{IIC} for mode II. Mixed-mode I/II fracture toughness has an effective value, as demonstrated by K_{eff}. Assuming a/R 0.3, the mode I and mode II dimensionless coefficients are B_I and B_{II}, respectively. When determining pure mode I, the crack angle is equal to zero to evaluate fracture toughness [21]. To determine the angle in pure mode II, the B_I variable in equation (2) needs to be changed to 0 first [31]. The experimental setup used for the Brazilian disc test is shown in Figure 6.

3. Results and Discussion

3.1. Compressive Strength. Figure 7 displays the results of an analysis of the compressive strength of geopolymer concrete constructed with fibers of varying lengths and types. Polypropylene fiber addition in geopolymer concrete significantly improved compressive strength by about 14.5 and 35.8% for G-SPF and G-LPF, respectively, compared to the
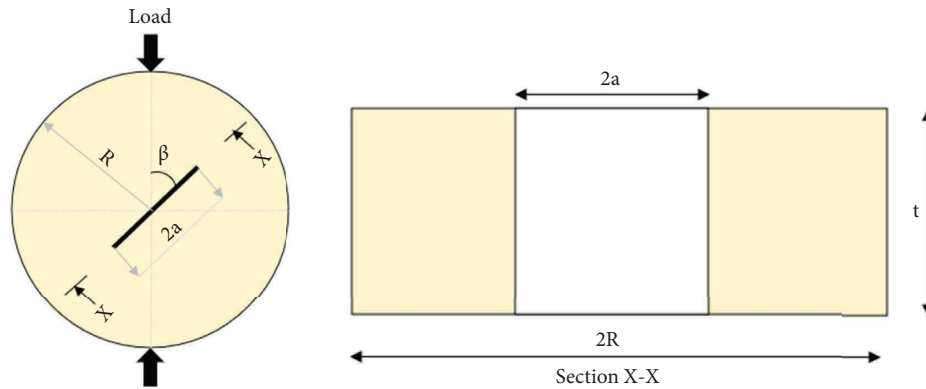
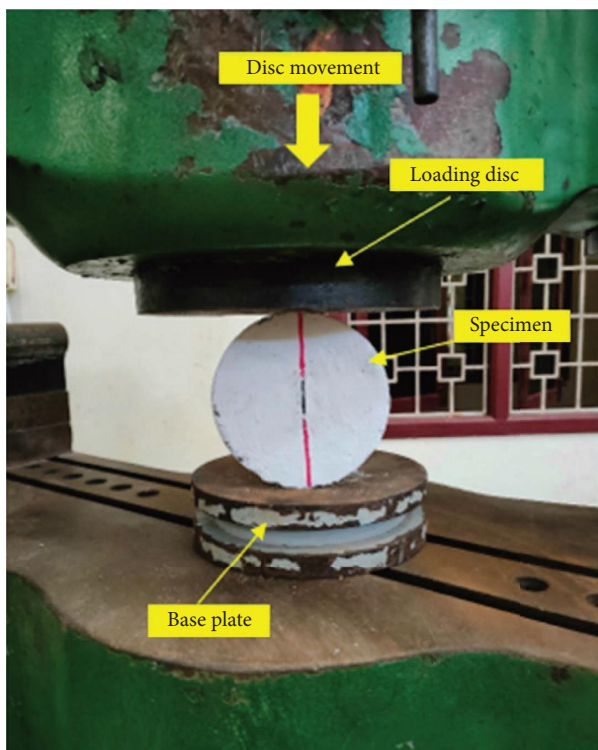FIGURE 5: Schematic of the Brazilian disc specimen with a center crack when subjected to compression.

FIGURE 6: Experimental setup.

initiation and development stages. Multiple studies showed that adding fibers increased the material's compressive strength [34, 35].

Adding short and long steel fibers to geopolymer concrete resulted in 50.1 and 73.9% improvements in compressive strength, respectively, as associated with the GPC specimen. A higher variation in compressive strength was seen between short and long fiber-based specimens, which tend to behave in a manner comparable to one another. In most cases, the potential of equally dispersed steel fibers is the primary reason for an inherent improvement in compressive strength [36]. This is because steel fibers tend to limit macrocrack developments. The stress is distributed more evenly throughout the concrete, cracks are less likely to spread rapidly, and bridging and reinforcing work together to slow the rate at which cracks grow [37]. The cracking progresses slowly in steel-fiber-based specimens throughout the fracturing phase, while polypropylene fibers form fast in randomly oriented and aligned specimens. The crack propagation appeared to be accompanied by louder fiber-pulling sounds in longer steel fiber specimens than in shorter ones. This suggests that more steel fibers span the crack region and control crack growth in the specimens with flexibly dispersed steel fibers. As a result, the specimen's strength and ductility are improved to a greater extent.

3.2. Analysis of Fracture Test Results. The load-carrying capacity of geopolymer specimens under different loading angles and the corresponding calculated fracture toughness are demonstrated in Table 4.

3.3. Analysis of Mode I Fracture Toughness of Geopolymer Concrete. The specimens of the Brazilian discs were subjected to diametral compressive loads at two different angles (0 and 90°) to evaluate fracture toughness. Consequently, with all these adjustments and changes, the specimens were presented with a mode I load situation. According to the results presented in Figure 8, the load-carrying capacity and fracture toughness were increased by adding fibers. For instance, adding short and long polypropylene fibers to the specimens (G-SPF and G-LPF) exhibited 1.41 and 1.52 times higher fracture toughness, respectively, compared to the
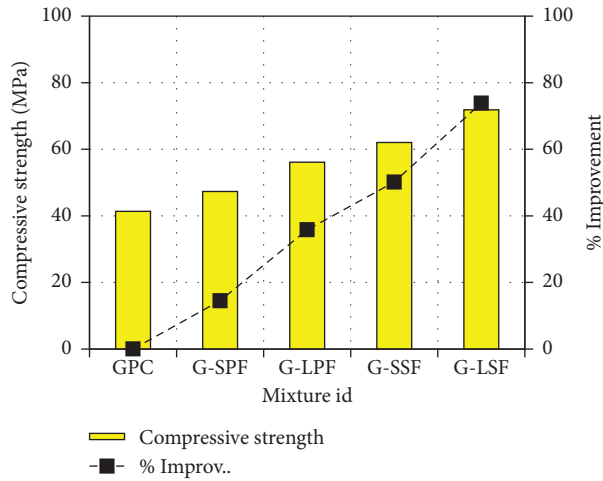
reference specimen (GPC). This behavior suggests that long polypropylene fibers significantly boost compressive strength compared to short fibers. This was since, when the fiber dosage was 1.5%, the concentration of short fibers in geopolymer concrete was considerable, causing the fiber not to be dispersed uniformly in the concrete [32]. Weak layer zones appeared in the specimens, which decreased the overall effectiveness of the short fiber on the geopolymer concrete specimen. Conversely, long polypropylene fibers were distributed uniformly and associated with higher tensile strength, resulting in a more remarkable improvement in compressive strength. The same behavior was noticed in an earlier study [33]. The incorporation of polypropylene fiber is responsible for the increased strength, and it stopped the cracking process in its tracks, both at the

FIGURE 7: Compressive strength of specimens.

TABLE 4: Fracture test results of nonfibrous and fibrous specimens.

Specimen Id	Loading angle (°)	Load (kN)	Fracture mode	The angle of crack initiation (°)	K_{IC} (MPa.m$^{1/2}$)	K_{IIC} (MPa.m$^{1/2}$)	K_{eff} (MPa.m$^{1/2}$)	Standard deviation
	0	11.23	I	0	0.26	0.00	0.26	0.03
	15	10.18	Mixed	20	−0.63	0.18	0.66	0.05
	28.83	10.55	II	32	0.00	0.45	0.45	0.03
GPC	45	9.40	Mixed	48	−0.31	0.41	0.51	0.05
	60	11.35	Mixed	64	−0.61	0.35	0.70	0.02
	75	11.88	Mixed	80	−0.77	0.11	0.77	0.03
	90	17.85	I	89	−0.89	0.00	0.89	0.05
	0	15.83	I	0	0.36	0.00	0.36	0.02
	15	14.23	Mixed	26	−0.46	0.63	0.77	0.01
	28.83	14.75	II	35	0.00	0.54	0.64	0.15
G-SPF	45	13.53	Mixed	50	0.22	−0.33	0.40	0.3
	60	15.40	Mixed	65	−0.63	−0.63	0.89	0.35
	75	16.03	Mixed	83	−0.97	0.32	1.03	0.02
	90	21.98	I	88	−1.10	0.00	1.10	0.01
	0	17.03	I	0	0.39	0.00	0.39	0.01
	15	15.48	Mixed	27	−0.91	−0.36	0.98	0.02
	28.83	16.00	II	38	0.00	0.44	0.44	0.05
G-LPF	45	14.73	Mixed	48	−0.48	0.64	0.80	0.02
	60	16.55	Mixed	68	−0.84	−0.56	1.01	0.025
	75	17.18	Mixed	86	−0.93	0.52	1.07	0.01
	90	23.23	I	90	−1.16	0.00	1.16	0.02
	0	26.10	I	0	0.60	0.00	0.60	0.03
	15	25.58	Mixed	20	−1.35	0.81	1.58	0.15
	28.83	24.38	II	35	0.00	0.90	0.90	0.10
G-SSF	45	24.43	Mixed	50	0.39	−0.60	0.71	0.20
	60	25.75	Mixed	67	−1.15	0.99	1.52	0.20
	75	25.68	Mixed	83	−1.56	0.52	1.65	0.25
	90	26.28	I	89	−1.31	0.00	1.31	0.10
	0	30.58	I	0	0.70	0.00	0.70	0.15
	15	28.93	Mixed	19	0.60	0.42	0.73	0.10
	28.83	28.18	II	42	0.00	0.88	0.88	0.05
G-LSF	45	25.95	Mixed	49	−1.52	−0.63	1.65	0.20
	60	27.75	Mixed	64	−1.49	0.85	1.72	0.10
	75	28.20	Mixed	86	−1.53	0.85	1.75	0.15
	90	30.73	I	90	−1.54	0.00	1.54	0.25

GPC (Figure 8(a)). The corresponding fracture toughness values were 0.36 and 0.39 MPa.m$^{1/2}$ (Figure 8(b)), respectively, while 0.26 MPa.m$^{1/2}$ was recorded for the GPC. The similar behavior was observed in the steel fiber specimens. The G-SSF and G-LSF specimens' load-carrying capacities increased by about 2.33 and 2.72 times, respectively. The calculated fracture toughness values for these two mixtures were 0.60 and 0.70 MPa.m$^{1/2}$, respectively. When the equivalent load was applied to the short fiber concrete, it was subjected to greater stress, which resulted in early crack formation, a lower load-carrying capacity, and excellent fracture toughness. This behavior could be attributed to the fact that each fiber in the network acts as a localized energy absorber with less effectiveness. The initial crack caused secondary cracks to emerge, spanned by short fibers that do not produce an efficient load transmission system. Fibrous geopolymer concrete is more resistant to cracking than nonfibrous concrete because its fibers impose tensile stress instead of compressive pressure during crack propagation [26]. They partially absorbed the energy and stopped the concrete from breaking further. As a result, the stress intensity at the crack tip is reduced, which inhibits the fracture in the specimen and causes the crack to follow a more challenging course, increasing the energy needed to pull the fibers out of the matrix [24].

Figures 8 and 9 depict that the failure load was typically observed to increase as the crack inclination angle increased from 0 to 90°. This behavior is due to the effectiveness of shear, and normal stress (tension) along the top and lower faces of the notched cracks was observed to rise as the crack angle of inclination increased [16]. It is observed from Figure 8(a) that the load-carrying capacity increased between 15.83 and 30.58 kN for the fibrous geopolymer concrete under 0°. These values ranged from 21.98 to 30.73 kN for the fibrous geopolymer concrete under 90°. The increment in fracture toughness of fibrous concrete under a crack inclination angle of 90° ranged from 1.40 to 2.84 times higher than the GPC specimen. However, the negative fracture toughness values were observed under a crack inclination angle of 90° due to the loading applied perpendicular to the notch length.

3.4. Analysis of Mode II Fracture Toughness of Geopolymer Concrete.

The mode II fracture phenomena of the geopolymer specimens are shown in Figure 10. When the loading angle was 28.83° with respect to the notch, it exhibited mode II fracture toughness. The load-carrying capacity for the GPC specimen was 10.55 kN, and the corresponding fracture toughness was 0.45 MPa.m$^{1/2}$. The load-carrying capacity was increased by 1.40 and 1.52 times for the G-SPF and G-LPF specimens, respectively, compared to the GPC. The fracture toughness (stress intensity factor) for these two mixtures was 0.54 and 0.64 MPa.m$^{1/2}$, respectively. It is clear from the above discussions that adding short polypropylene fiber exhibited less performance in ultimate load and fracture toughness under pure mode II compared to long polypropylene fibers. At the same time, adding steel fibers exhibited excellent performance in the

load-carrying capacity by 2.31 and 2.67 for the short and long steel fibrous specimens (G-SSF and G-LSF), respectively. This behavior is due to the fiber and composite matrix bonding methods contributing to higher fracture strength improvement under mode II. As a result of the formation of an elastic shearing bond and the fiber bearing, the fibers can withstand pull-out forces. These two mechanisms are also known, respectively, as anchoring and adhesion [38]. The elastic shear bond's maximum strain is low and would peak rather rapidly if pull-out behavior started. Nevertheless, fiber bearing has a more profound effect because it is predicated on elementary fiber qualities like aspect ratios and strength under tensile loads [39]. With a matrix providing uniform bond strength to all specimens, the mechanism's activity can be precisely defined by adjusting these two variables. Once the elastic shear link between the composite matrix and fiber diminishes, a distorted zone forms around the fiber and anchorage ensues. This procedure will remain until the load applied to the fiber is greater than its yield strength [40]. At this particular position, the fibers experience local deformations. Since the failure of the matrix depends on its tensile strain limit, this could also lead to its failure. This phenomenon was seen clearly in long fiber-based geopolymer specimens.

3.5. Analysis of Mixed-Mode (I/II) Fracture Toughness of Geopolymer Concrete.

This research has demonstrated that the fracture toughness of geopolymer concrete in pure and mixed modes was measured using the notched cracked Brazilian disc specimen. The stress intensity factor is a quicker and more accessible alternative to other complex testing methods by changing the orientation of the crack to align with the load being applied. Therefore, this study's unique and original mixed-mode fracture toughness test results may be crucial information for the designers and manufacturers of concrete structures. The changes in fracture toughness under mixed modes (15°, 45°, 60°, and 75°) for geopolymer concrete are shown in Figures 11–14. It is observed from the figures that the load-carrying capacity values were increased by adding both short and long fibers. Compared with the GPC specimen, the load-carrying capacity of the G-SPF and G-LPF specimens under a 15° loading angle was increased by 1.40 and 1.52 times, respectively. Similarly, the G-SSF and G-LSF specimens exhibit improvements in the load-carrying capacity by about 2.51 and 2.58 times, respectively. The calculated fracture toughness ranged from 0.77 to 1.58 MPa.m$^{1/2}$. This group observed the highest fracture toughness in the G-SSF specimen (Figure 11). Besides, the G-LSF specimen exhibited a higher load-carrying capacity, and the fracture toughness under a 15° loading angle is lower than that of the other fibrous specimens.

Under a 45° loading angle, the G-SPF and G-LPF specimens' load-carrying capacities were 1.44 and 1.57 times that of the GPC specimen, respectively. Similarly, the load-carrying capacity of the G-SSF and G-LSF specimens improves by approximately 2.51 and 2.58 times, respectively, when compared to the GPC. The fracture toughness under a 45° loading
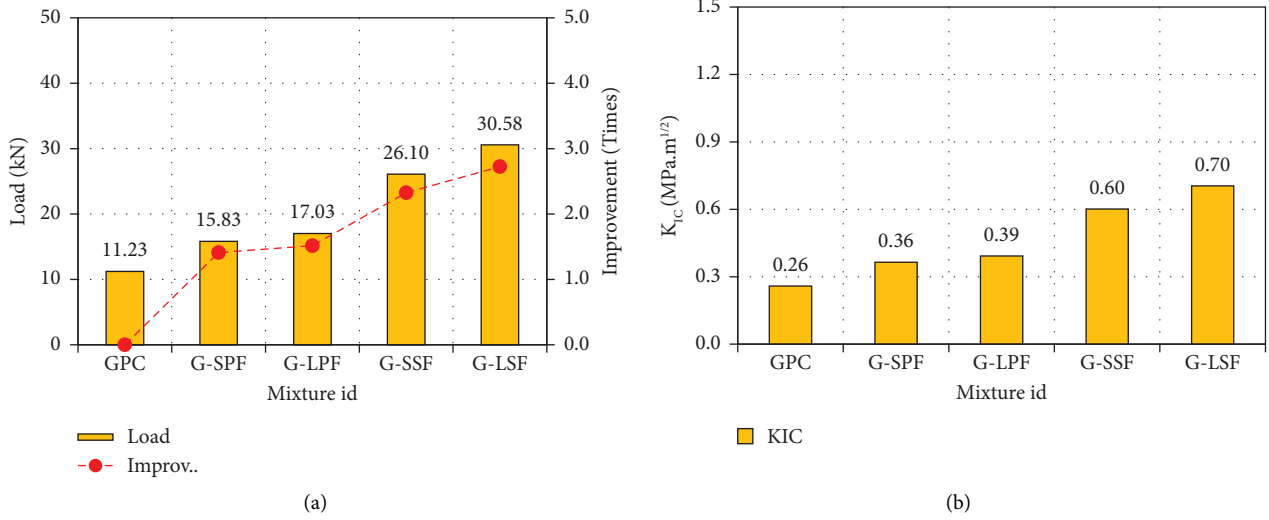
(a)

(b)

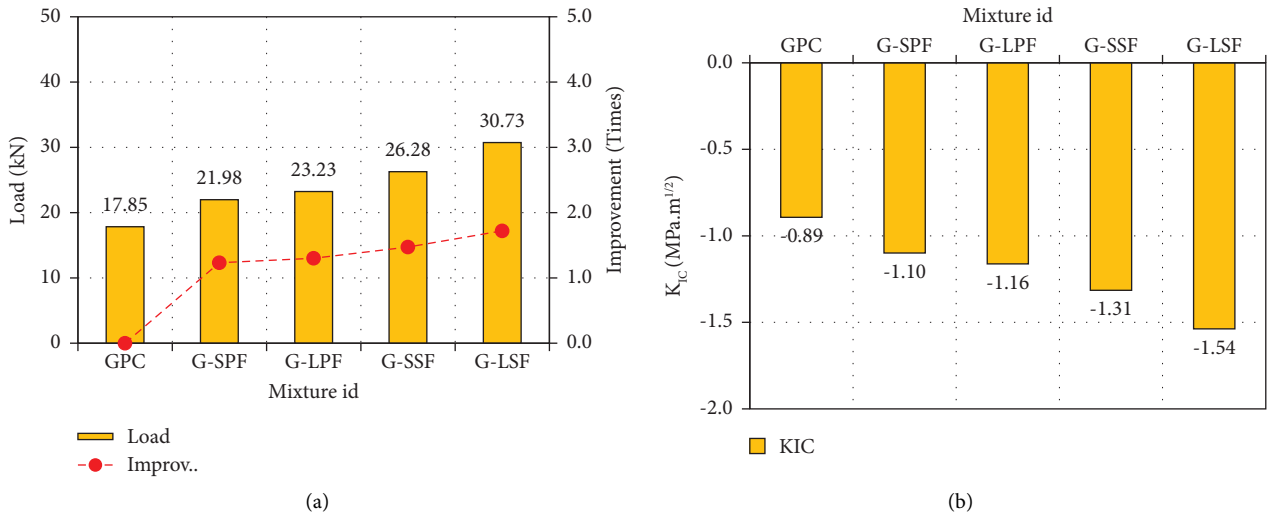FIGURE 8: Mode I fracture toughness of specimens under 0° loading.

(a)

(b)

FIGURE 9: Mode I fracture toughness of specimens under 90° loading.
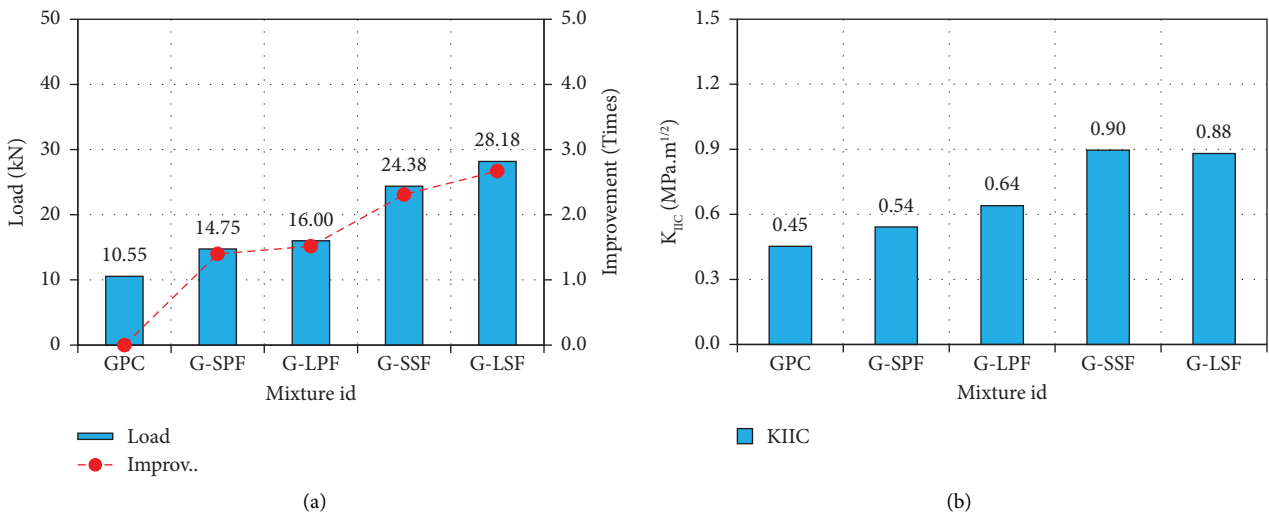

(a)

(b)

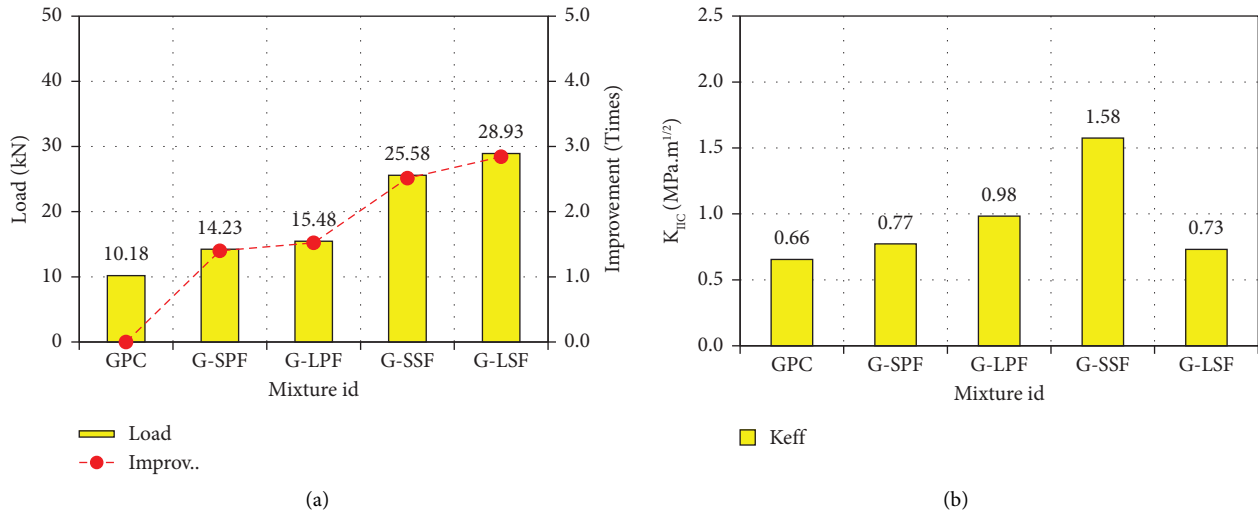FIGURE 10: Mode II fracture toughness of specimens under 28.83° loading.

(a)

(b)

FIGURE 11: Mixed-mode fracture toughness of specimens under 15° loading.
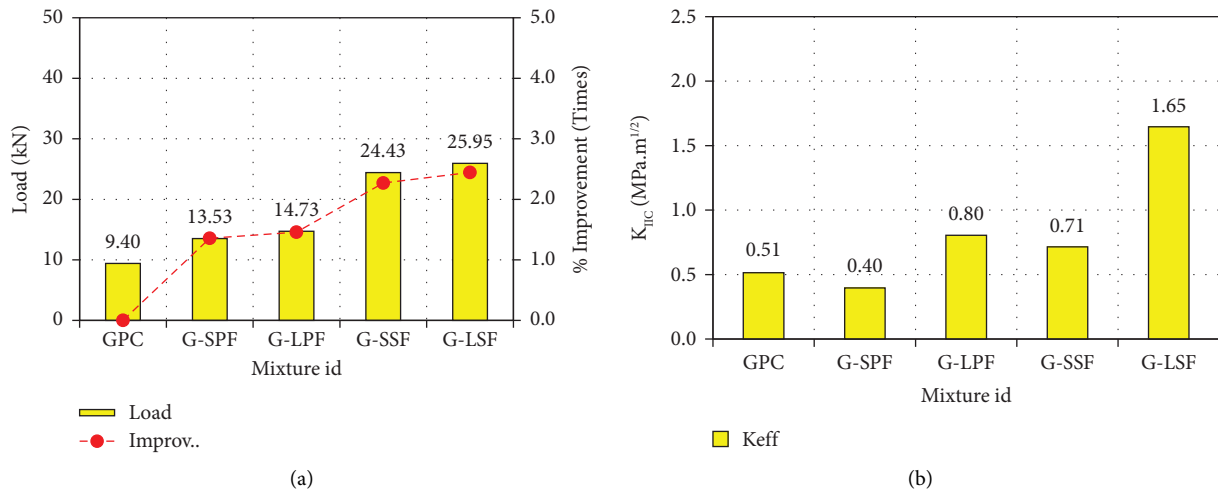

(a)

(b)

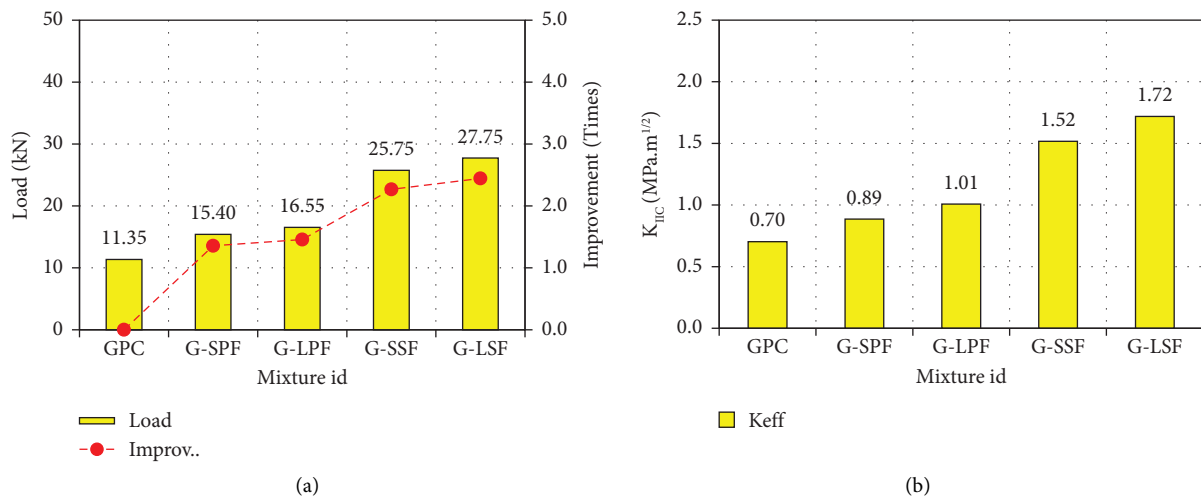FIGURE 12: Mixed-mode fracture toughness of specimens under 45° loading.

(a)

(b)

FIGURE 13: Mixed-mode fracture toughness of specimens under 60° loading.
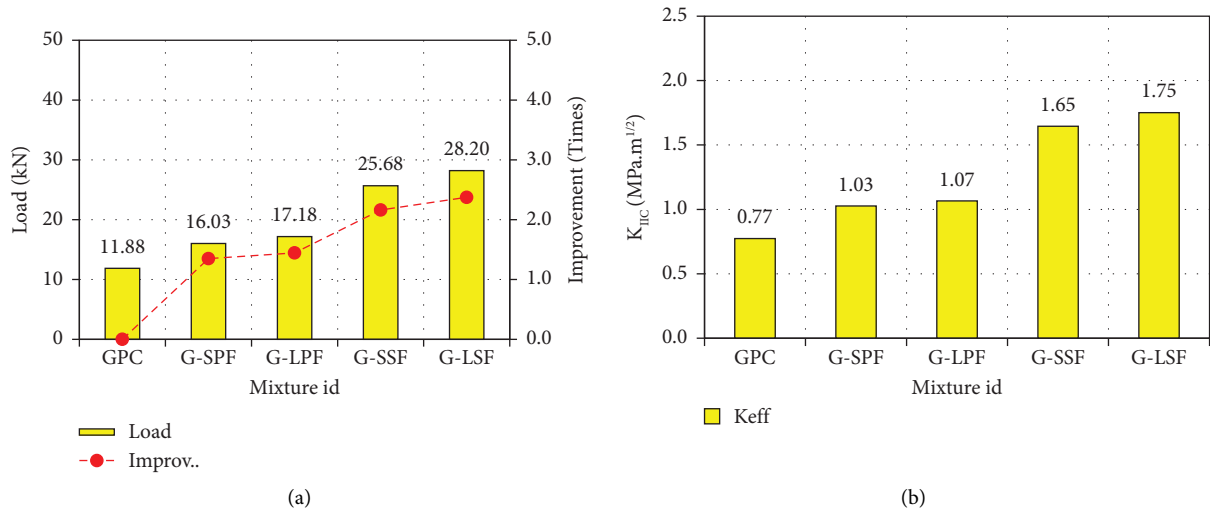
(a)

(b)

FIGURE 14: Mixed-mode fracture toughness of specimens under 75° loading.

(a)

(b)
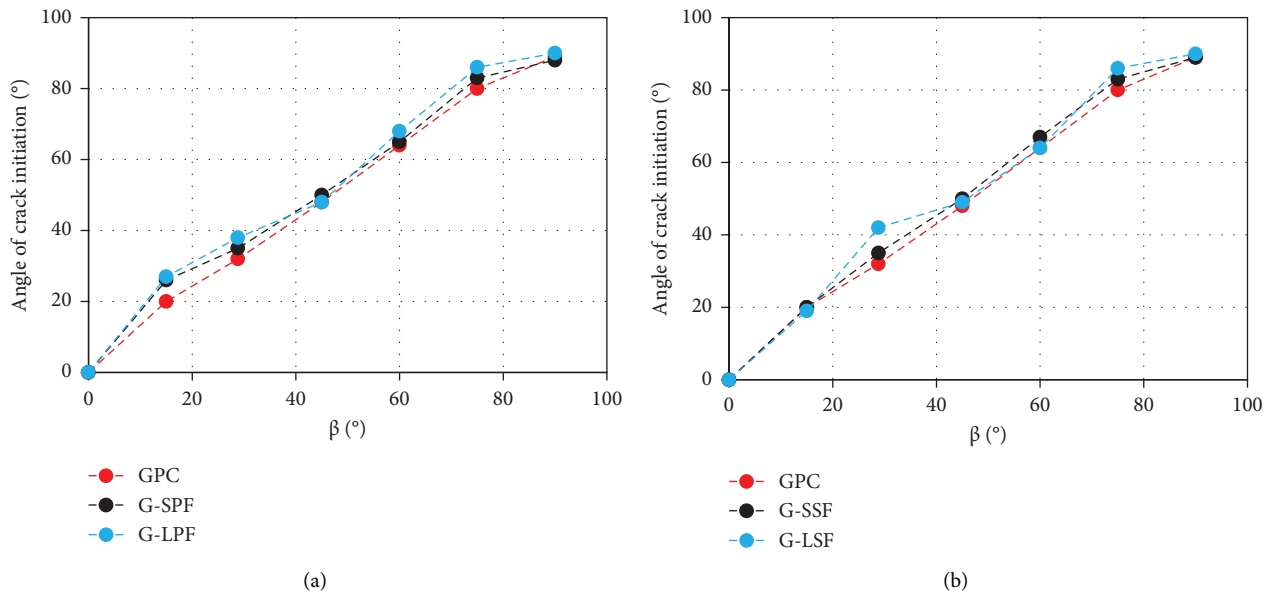
FIGURE 15: The relationship between the angle of crack initiation and β.

angle was significantly lower for all specimens when compared to a loading angle of 15° (Figure 12). The same behavior was observed in the other two loading angles (60° and 75°). The load-carrying capacity improvement for the specimens under these two loading angles ranged from 1.6 to 2.37 times higher. The corresponding fracture toughness values ranged from 0.70 to 1.75 MPa.m$^{1/2}$ (Figures 13 and 14). Nevertheless, the behavior of geopolymer fibrous concrete under modes I and II is mirrored in the mixed mode. As individual fibers operate as little tensile elements in their effective local zone, they inhibit the concrete from cracking at these points. The preceding considerations have made it abundantly evident that the mixed-mode fracture toughness is more critical in 28.83° and 45° than in 60° and 75°. When compared to polypropylene fibers, steel fibers perform exceptionally well in improving fracture toughness in mixed modes [38].

3.6. Angle of Crack Initiation and Loading Angle Relationship. Figure 15 illustrate the connection between the loading direction and the crack-originated angle for the tested geopolymer fibrous concrete. It can be seen from Figure 15 that a greater crack commencement angle is related to the increased loading angle with respect to the notch angle. At an angle of inclination of 60° or less, crack propagation started at the crack's tip, which had already formed. If the wing's angle exceeds 75 degrees, the crack will spread outward from its origin (Figures 16 and 17). This angle will ultimately approach 90° as the loading angle increases and the crack assumes a horizontal path. This pattern agrees with the findings found in the scientific literature [21]. Recent research in this area includes a study conducted by Xiankai et al. [41], which can be referenced as one of the available options. As per research findings, the maximum crack
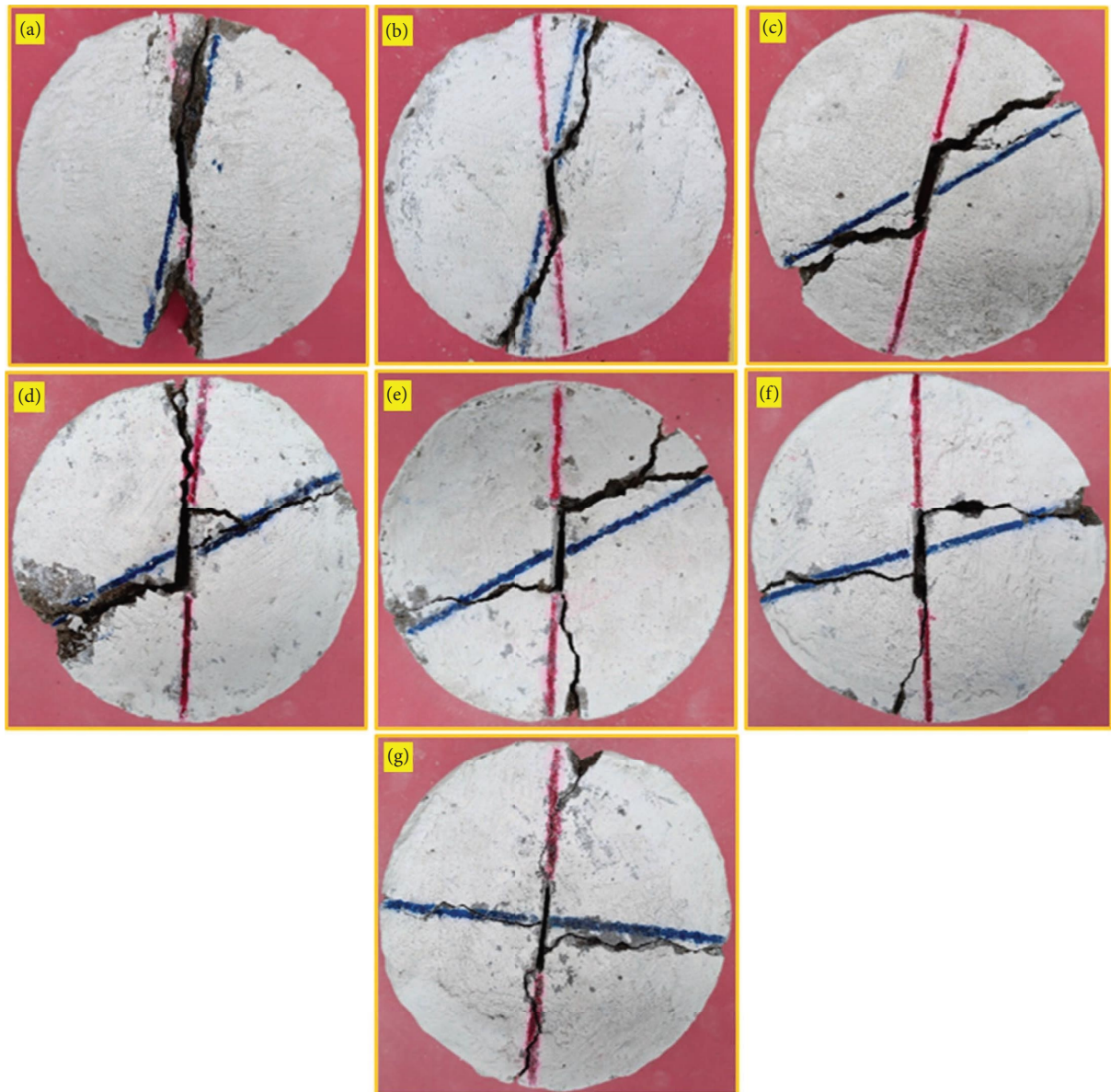
FIGURE 16: Fracture of nonfibrous specimens at different loading angles: (a) 0°, (b) 15°, (c) 28.83°, (d) 45°, (e) 60°, (f) 75°, and (g) 90°.

initiation angle occurs at 90° with respect to the notch when the specimen is subjected to the 90° loading angle. According to Bobet and Einstein's [42] research, cracks typically form parallel to the direction of the load. Moreover, the cracks in the wings follow a curved pattern on their way to the loading point. An intriguing finding of this research is that, regardless of the fiber type and dosage, wing cracks expand in a curved pattern and eventually align themselves with the direction of loading. As a result, the fibrous specimens had a greater crack initiation angle than the nonfibrous geopolymer specimens.

3.7. Fracture Pattern. When comparing fracture occurrences among experimental groups, there were noticeable differences in nonfibrous and fibrous geopolymer concrete. All specimen cracks were found to have originated at the crack tip and spread outward toward the loading position. Other studies observe this type of cracking pattern [43]. None of the cracks rotated out of a plane, and the fracture surfaces were quite curved for the nonfibrous specimens at different loading angles (shown in Figures 16(a)–16(g)). Every nonfibrous specimen under different angles showed curved open surfaces with
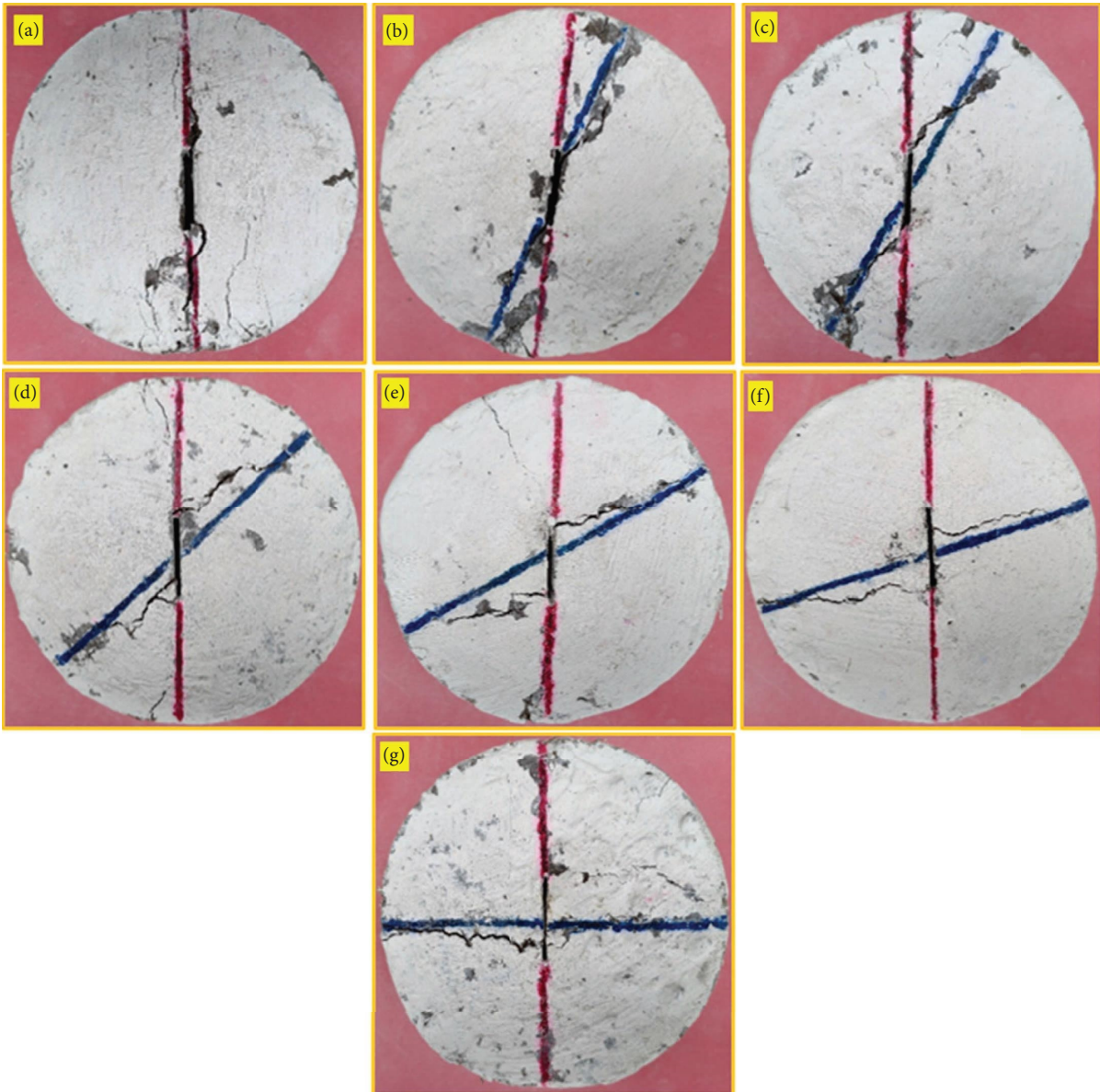
FIGURE 17: Fracture of short steel fibrous specimens at different loading angles: (a) 0°, (b) 15°, (c) 28.83°, (d) 45°, (e) 60°, (f) 75°, and (g) 90°.

fractured patterns that reached from the crack's tip to the loading location [24]. Permanent deformation and small cracks are recorded on the fracture surface as they grow and eventually break into two pieces, which signifies the brittle behavior. The nonfibrous geopolymer concrete behaved brittlely when subjected to the different loading angles. At the point of failure, none of the fibrous geopolymer specimens fragmented into two separate pieces, regardless of the inclination loading angle (shown in Figures 17 and 18(a)–18(g)). This behavior arises due to the fiber's capacity to preserve the disc specimens' structural integrity under various loading circumstances [21]. This assures that the fractured parts will interlock owing to their crack-inhibiting and bridging abilities, ultimately failing with a combination of a large crack and numerous smaller cracks [44].
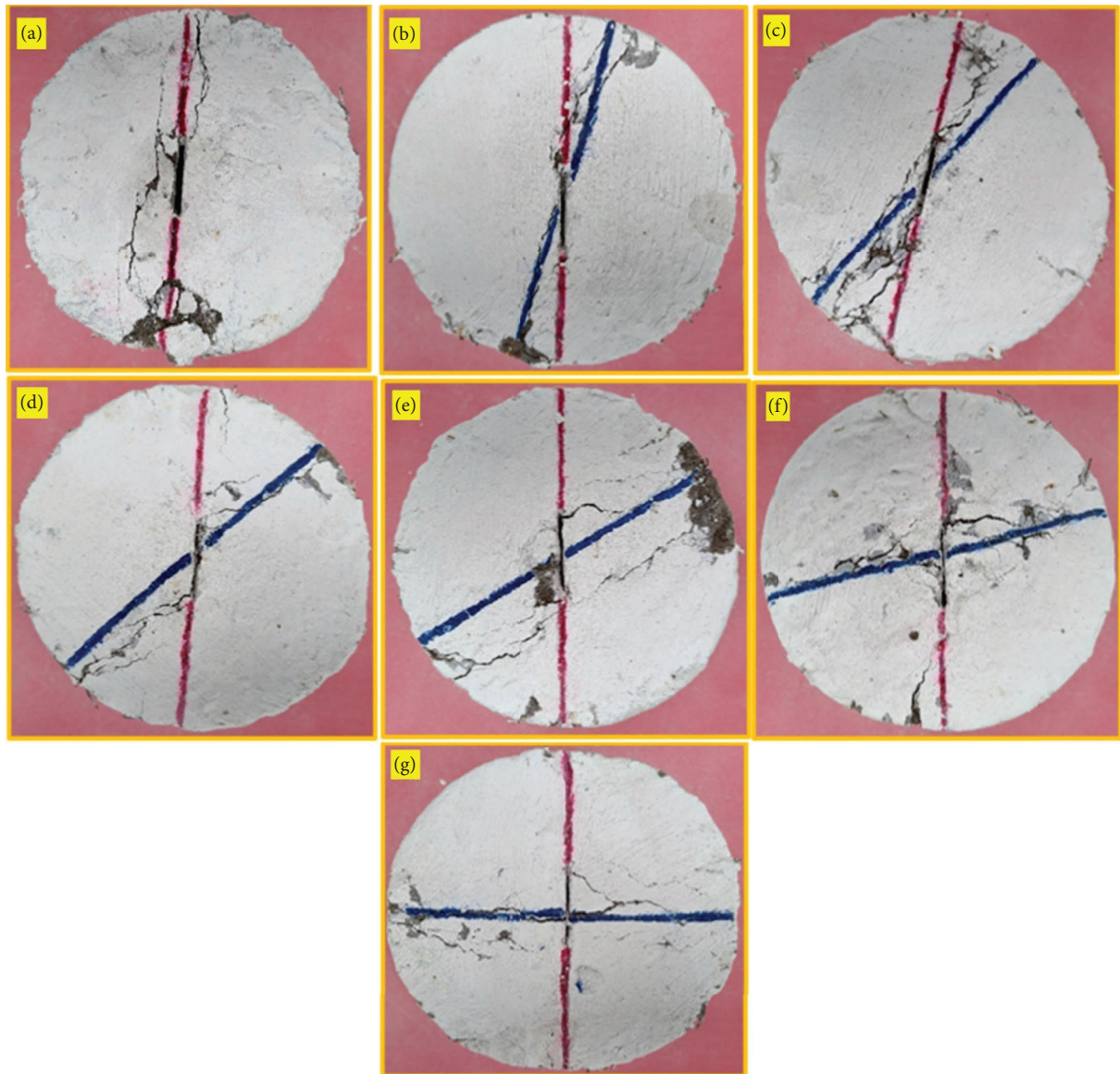
FIGURE 18: Fracture of long steel fibrous specimens at different loading angles: (a) 0°, (b) 15°, (c) 28.83°, (d) 45°, (e) 60°, (f) 75°, and (g) 90°.

3.8. Scanning Electron Microscope. The scanning electron micrograph images of the geopolymer matrix are depicted in Figure 19. Various magnifications were used to inspect the GPC specimen's fracture surfaces. Figure 19 illustrates an agglomerate particle break associated with a crack at magnifications of 20 and 100 μm, respectively. Moreover, the crack is stopped at contact with the geopolymeric matrix, which is evidence of the material's exceptional fracture toughness. Figure 19 also reveals the presence of fibrous CaO-SiO$_2$-H$_2$O (C-S-H) crystals, which play a role in the geopolymer's overall reinforcement. Since the fibers that are pulled out of their cavities will now occupy the interface, the prevalence of fibers predicts that this phenomenon will increase. The presence of spaces and grooves (residue from fiber pull-out) in the geopolymer matrix corroborates this finding. A "fiber fossil" could be identified as a remnant of the porous layer present at the matrix-fiber interface.
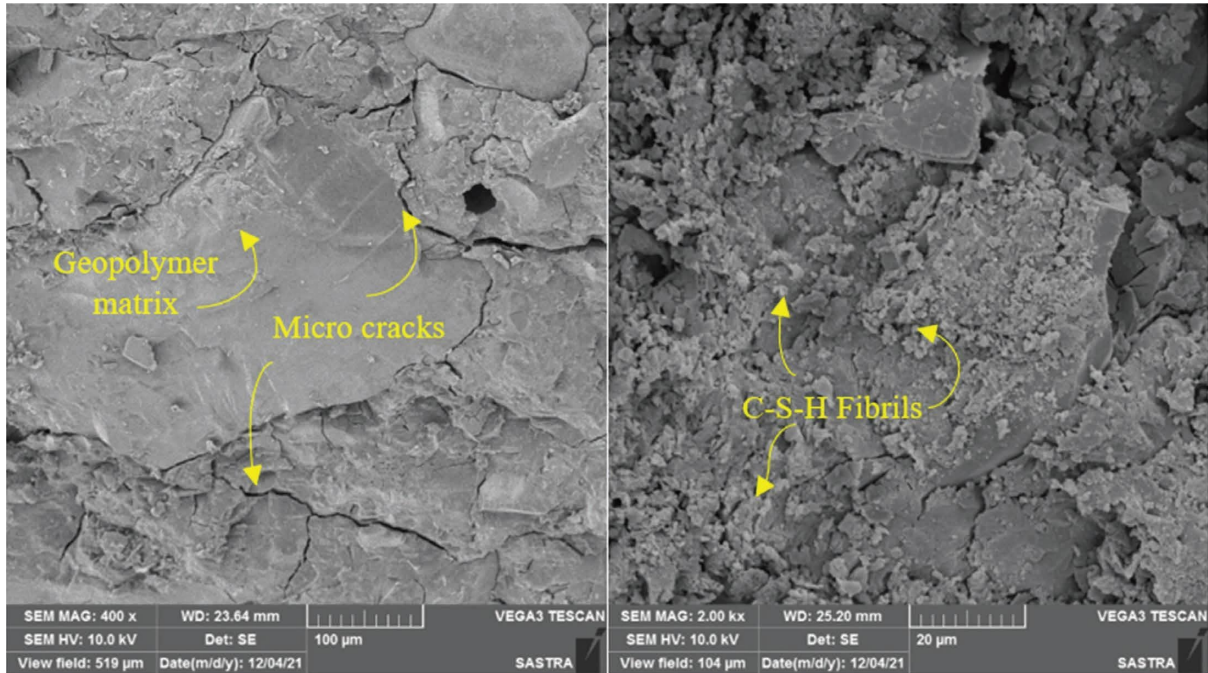
FIGURE 19: Scanning electron microscope of the geopolymer matrix.

4. Conclusions

This study tested geopolymer concrete with various fibers for its crack propagation and fracture toughness by employing a fractured Brazilian disc. The crack growth analysis for fractured specimens and the determination of fracture toughness for I, II, and I/II fracture modes were conducted. The following primary findings may be deduced from the data collected during the experiments:

(1) The compressive strength was increased by roughly 14.5% for G-SPF and 35.8% for G-LPF when polypropylene fibers were added to geopolymer concrete. Similarly, the compressive strength increased by 50.1% and 73.9%, respectively, after short and long steel fibers were added to geopolymer concrete (G-SSF and G-LSF). In specimens under compression, the cracking progresses slowly in steel fiber-based specimens throughout the fracturing phase, while polypropylene fibers form quickly in randomly oriented and aligned specimens. The performance of steel and long fibers exhibited better compressive strength than the short and polypropylene fibers.

(2) The fracture toughness values for all geopolymer concrete specimens under various loading angles ranged from 0.26 to 0.70 MPa.m$^{1/2}$ for 0°, 0.66 to 1.58 MPa.m$^{1/2}$ for 15°, 0.45 to 0.90 MPa.m$^{1/2}$ for 28.83°, 0.51 to 1.65 MPa.m$^{1/2}$ for 45°, 0.70 to 1.72 MPa.m$^{1/2}$ for 60°, 0.77 to 1.75 MPa.m$^{1/2}$ for 75°, and 0.89 to 1.54 MPa.m$^{1/2}$ for 90°. Compared to long fibers, the addition of short fiber resulted in inferior performance in terms of ultimate load and fracture toughness across all three modes. Besides, increasing the loading angle increased the load-carrying capacity values.

(3) The mixed mode of geopolymer fiber concrete exhibits the same characteristics as modes I and II. In their localized effective zone, individual fibers function as small tensile elements, preventing the concrete from cracking. The mixed-mode fracture toughness is more important at 28.83° and 45° than at 60° and 75°.

(4) The crack tip initiated crack propagation at 60° or less inclination. The crack will grow outward from its source when the wing is angled at more than 75 degrees. As the loading angle increases and the crack continues along a horizontal trajectory, this angle will eventually approach 90°.

(5) As the crack angle increased from 0 to 45°, the force needed to break the specimens reduced; however, the opposite was true as the crack angle increased from 45 to 90°. All specimen cracks were determined to have started at the crack tip and propagated out toward the loading point. At any of the loading angles, not a single crack rotated out of its plane, and the fracture surfaces of the nonfibrous specimens were highly curved.

Data Availability

Data are available upon request.

Conflicts of Interest

The authors declare that they have no conflicts of interest regarding the publication of this paper.

Acknowledgments

References

[1] M. F. Zawrah, H. A. Badr, R. M. Khattab, H. E. H. Sadek, S. E. Abo Sawan, and A. A. El-Kheshen, "Fabrication and characterization of non-foamed and foamed geopolymers from industrial waste clays," *Ceramics International*, vol. 47, no. 20, pp. 29320–29327, 2021.

[2] N. Akhtar, T. Ahmad, D. Husain et al., "Ecological footprint and economic assessment of conventional and geopolymer concrete for sustainable construction," *Journal of Cleaner Production*, vol. 380, Article ID 134910, 2022.

[3] M. Amin, Y. Elsakhawy, K. Abu el-hassan, and B. A. Abdelsalam, "Behavior evaluation of sustainable high strength geopolymer concrete based on fly ash, metakaolin, and slag," *Case Studies in Construction Materials*, vol. 16, Article ID e00976, 2022.

[4] F. A. Shilar, S. V. Ganachari, V. B. Patil, and K. S. Nisar, "Evaluation of structural performances of metakaolin based geopolymer concrete," *Journal of Materials Research and Technology*, vol. 20, pp. 3208–3228, 2022.

[5] S. Oyebisi, F. Olutoge, P. Kathirvel et al., "Sustainability assessment of geopolymer concrete synthesized by slag and corncob ash," *Case Studies in Construction Materials*, vol. 17, Article ID e01665, 2022.

[6] P. Kathirvel and S. Sreekumaran, "Sustainable development of ultra high performance concrete using geopolymer technology," *Journal of Building Engineering*, vol. 39, Article ID 102267, 2021.

[7] H. S. Rajan and P. Kathirvel, "Sustainable development of geopolymer binder using sodium silicate synthesized from agricultural waste," *Journal of Cleaner Production*, vol. 286, Article ID 124959, 2021.

[8] N. Arunachelam, J. Maheswaran, M. Chellapandian, and T. Ozbakkaloglu, "Effective utilization of copper slag for the production of geopolymer concrete with different NaOH molarity under ambient curing conditions," *Sustainability*, vol. 14, no. 23, Article ID 16300, 2022.

[9] N. Arunachelam, J. Maheswaran, M. Chellapandian, G. Murali, and N. I. Vatin, "Development of high-strength geopolymer concrete incorporating high-volume copper slag and micro silica," *Sustainability*, vol. 14, no. 13, p. 7601, 2022.

[10] G. Murali, J. Venkatesh, N. Lokesh, T. R. Nava, and K. Karthikeyan, "Comparative experimental and analytical modeling of impact energy dissipation of ultra-high performance fibre reinforced concrete," *KSCE Journal of Civil Engineering*, vol. 22, no. 8, pp. 3112–3119, 2018.

[11] V. R. Ramkumar, K. Chinnaraju, and G. Murali, "On low-energy impact response of fibre reinforced concrete made with binary and quaternary cementitious blends of lime sludge, fly ash and metakaolin," *Revista Romana de Materiale/Romanian Journal of Materials*, vol. 47, 2017.

[12] A. Sheta, X. Ma, Y. Zhuge, M. ElGawady, J. Mills, and E. Abd-Elaal, "Flexural strength of innovative thin-walled composite cold-formed steel/PE-ECC beams," *Engineering Structures*, vol. 267, Article ID 114675, 2022.

[13] S. Ahmed, M. Xing, Z. Yan, M. ElGawady, J. E. Mills, and E. Abdelaal, "Shear behaviour of thin-walled composite cold-formed steel/PE-ECC beams," *Steel and Composite Structures*, vol. 46, no. 1, 2023.

[14] A. Sheta, X. Ma, Y. Zhuge, M. ElGawady, J. E. Mills, and E. Abd-Elaal, "Axial compressive behaviour of thin-walled composite columns comprise high-strength cold-formed steel and PE-ECC," *Thin-Walled Structures*, vol. 184, Article ID 110471, 2023.

[15] G. Murali and E. Vinodha, "Experimental and analytical study of impact failure strength of steel hybrid fibre reinforced concrete subjected to freezing and thawing cycles," *Arabian Journal for Science and Engineering*, vol. 43, no. 10, pp. 5487–5497, 2018.

[16] N. Erarslan, "Analysing mixed mode (I-II) fracturing of concrete discs including chevron and straight-through notch cracks," *International Journal of Solids and Structures*, vol. 167, pp. 79–92, 2019.

[17] B. N. Whittaker, R. N. Singh, and G. Sun, *Rock Fracture Mechanics-Principles, Design and Applications*, Elsevier, Amsterdam, Netherlands, 1992.

[18] A. Carpinteri, G. Lacidogna, and F. Accornero, "Evolution of the fracturing process in masonry arches," *Journal of Structural Engineering*, vol. 141, no. 5, Article ID 04014132, 2015.

[19] R. W. Margevicius, J. Riedle, and P. Gumbsch, "Fracture toughness of polycrystalline tungsten under mode I and mixed mode I/II loading," *Materials Science and Engineering A*, vol. 270, no. 2, pp. 197–209, 1999.

[20] M. R. M. Aliha and M. R. Ayatollahi, "Rock fracture toughness study using cracked chevron notched Brazilian disc specimen under pure modes I and II loading - a statistical approach," *Theoretical and Applied Fracture Mechanics*, vol. 69, pp. 17–25, 2014.

[21] M. Hatami Jorbat, M. Hosseini, and M. Mahdikhani, "Effect of polypropylene fibers on the mode I, mode II, and mixed-mode fracture toughness and crack propagation in fiber-reinforced concrete," *Theoretical and Applied Fracture Mechanics*, vol. 109, Article ID 102723, 2020.

[22] M. R. M. Aliha and M. R. Ayatollahi, "Mixed mode I/II brittle fracture evaluation of marble using SCB specimen," *Procedia Engineering*, vol. 10, pp. 311–318, 2011.

[23] M. Ghomian and M. Dehestani, "In-plane modes of fracture and effective parameters of self-consolidating concrete," *Journal of Materials in Civil Engineering*, vol. 31, no. 8, 2019.

[24] A. Razmi and M. M. Mirsayar, "On the mixed mode I/II fracture properties of jute fiber-reinforced concrete," *Construction and Building Materials*, vol. 148, pp. 512–520, 2017.

[25] S. Sreenath, K. S. R. Mohan, and G. Murali, "Fracture toughness of reactive powder fibrous concrete composites under pure and mixed modes (I/III)," *Buildings*, vol. 12, no. 5, p. 599, 2022.

[26] N. P. Asrani, G. Murali, H. S. Abdelgader, K. Parthiban, M. K. Haridharan, and K. Karthikeyan, "Investigation on mode I fracture behavior of hybrid fiber-reinforced geopolymer composites," *Arabian Journal for Science and Engineering*, vol. 44, no. 10, pp. 8545–8555, 2019.

[27] C. Astm, "Specification for Fly Ash and Raw or Calcined Natural Pozzolan for Use as a mineral Admixture in Portland Cement Concrete," Astm, 1991, https://webstore.ansi.org/standards/astm/astmc61803.

[28] S. Karthik and K. S. R. Mohan, "A taguchi approach for optimizing design mixture of geopolymer concrete incorporating fly ash, ground granulated blast furnace slag and silica fume," *Crystals*, vol. 11, p. 1279, 2021.

[29] IS 383, *Coarse and fine Aggregate for concrete - Specification (Third Revision)*, IS 383, 2016.

[30] H. Awaji and S. Sato, "Combined mode fracture toughness measurement by the disk test," *Journal of Engineering Materials and Technology*, vol. 100, no. 2, pp. 175–182, 1978.

[31] G. R. Krishnan, X. L. Zhao, M. Zaman, and J. C. Roegiers, "Fracture toughness of a soft sandstone," *International Journal of Rock Mechanics and Mining Sciences*, vol. 35, no. 6, pp. 695–710, 1998.

[32] N. Balgourinejad, M. Haghighifar, R. Madandoust, and S. Charkhtab, "Experimental study on mechanical properties, microstructural of lightweight concrete incorporating polypropylene fibers and metakaolin at high temperatures," *Journal of Materials Research and Technology*, vol. 18, pp. 5238–5256, 2022.

[33] S. Karthik, K. S. R. Mohan, and G. Murali, "Investigations on the response of novel layered geopolymer fibrous concrete to drop weight impact," *Buildings*, vol. 12, no. 2, p. 100, 2022.

[34] A. S. M. Akid, S. Hossain, M. I. U. Munshi et al., "Assessing the Influence of Fly Ash and Polypropylene Fiber on Fresh, Mechanical and Durability Properties of concrete," *Journal of King Saud University - Engineering Sciences*, 2021.

[35] G. Murali, N. Prasad, S. Klyuev et al., "Impact resistance of functionally layered two-stage fibrous concrete," *Fibers*, vol. 9, no. 12, p. 88, 2021.

[36] N. Prasad and G. Murali, "Research on flexure and impact performance of functionally-graded two-stage fibrous concrete beams of different sizes," *Construction and Building Materials*, vol. 288, Article ID 123138, 2021.

[37] T. Abirami, M. Loganaganandan, G. Murali et al., "Experimental research on impact response of novel steel fibrous concretes under falling mass impact," *Construction and Building Materials*, vol. 222, pp. 447–457, 2019.

[38] G. Murali, S. R. Abid, N. I. Vatin, M. Amran, and R. Fediuk, "Influence of height and weight of drop hammer on impact strength and fracture toughness of two-stage fibrous concrete comprising nano carbon tubes," *Construction and Building Materials*, vol. 349, Article ID 128782, 2022.

[39] M. P. Salaimanimagudam, C. R. Suribabu, G. Murali, and S. R. Abid, "Impact response of hammerhead pier fibrous concrete beams designed with topology optimization," *Periodica Polytechnica: Civil Engineering*, vol. 64, pp. 1244–1258, 2020.

[40] R. Rithanyaa, G. Murali, M. P. Salaimanimagudam, R. Fediuk, H. S. Abdelgader, and A. Siva, "Impact response of novel layered two stage fibrous composite slabs with different support type," *Structures*, vol. 29, pp. 1–13, 2021.

[41] B. Xiankai, T. Meng, and Z. Jinchang, "Study of mixed mode fracture toughness and fracture trajectories in gypsum interlayers in corrosive environment," *Royal Society Open Science*, vol. 5, 2018.

[42] A. Bobet and H. H. Einstein, "Fracture coalescence in rock-type materials under uniaxial and biaxial compression," *International Journal of Rock Mechanics and Mining Sciences*, vol. 35, no. 7, pp. 863–888, 1998.

[43] X. Pan, J. Huang, Z. Gan, W. Hua, and S. Dong, "Investigation on mixed-mode II-III fracture of the sandstone by using eccentric cracked disk," *Theoretical and Applied Fracture Mechanics*, vol. 115, Article ID 103077, 2021.

[44] D. Scorza, C. Ronchei, S. Vantadori, and A. Zanichelli, "Size-effect independence of hybrid fiber-reinforced roller-compacted concrete fracture toughness," *Composites Part C: Open Access*, vol. 9, Article ID 100306, 2022.